International Journal of Mechanical and Production Engineering Research and Development (IJMPERD)
ISSN (P): 2249-6890; ISSN (E): 2249-8001
Vol. 9, Issue 4, Aug 2019, 731-744
© TJPRC Pvt. Ltd.

IMMOBILIZED PAni-TiO_2 NANO-PHOTOCATALYST MODELING FOR PHOTOCATALYTIC DEGRADATION OF 1, 2-DICHLOROETHANE USING RESPONSE SURFACE METHODOLOGY (RSM) AND ARTIFICIAL NEURAL NETWORK (ANN)

MAHDI MOHSENZADEH[1], SEYED AHMAD MIRBAGHERI[2] & SAMADSABBAGHI[3]

[1]*Research Scholar, Department of Environmental Engineering, Faculty of Civil Engineering, K. N. Toosi University of Technology, Mirdamad intersection, Valiasr Ave, Tehran, Iran*

[2]*Professor, Department of Environmental Engineering, Faculty of Civil Engineering, K. N. Toosi University of Technology, Mirdamad intersection, Valiasr Ave, Tehran, Iran*

[3]*Associate Professor, Department of Nano Chemical Engineering, Faculty of Advanced Technologies, Shiraz University, Shiraz, Iran*

ABSTRACT

Heterogeneous photocatalytic degradation as an advanced oxidation process (AOP) is a complicated process, because many independent influential parameters can affect degradation efficiency as the response of the system. Therefore, they are difficult to be modelled using conventional mathematical modelling. This leads to uncertainty in the design and built of industrial scale photocatalytic reactors. In this study, heterogeneous photocatalytic degradation of 1,2-dichloroethane using immobilized PAni-TiO2 nano-photocatalyst was modeled by Response Surface Methodology (RSM) and Artificial Neural Network (ANN) techniques and the results were compared. Central Composite Design (CCD) was used for design of experiments. Two independent parameters of catalyst loading and catalyst composition were considered as independent parameters and 1,2-DCE degradation was considered as the response parameter. RSM suggested a quadratic model by verifying lack of fit, model summary statistics and analysis of variance (ANOVA) statistics. ANN model with different structures were developed, trained, validated and tested. The results showed that both models predicted the photocatalytic degradation of 1,2-DCE with high precision. However, the ANN model had a slightly better performance. The optimal ANN model with tansig activation function, BR training function and 2-2-1 structure was the best model for prediction of 1,2-DCE photocatalytic degradation. The design expert software optimized 1,2-DCE removal (71.42%) by optimizing independent parameters of catalyst loading and catalyst composition at 0.4 mg/cm^2 and 2.4 [TiO_2:PAni], respectively.

KEYWORDS: Immobilized PAni-TiO_2, 1, 2-Dichloroethane, Modeling, Response Surface Methodology & Artificial Neural Network

Received: May 08, 2019; **Accepted**: May 28, 2019; **Published**: Jul 08, 2019; **Paper Id**.: IJMPERDAUG201973

1. INTRODUCTION

1, 2-Dichloroethane (1,2-DCE)is a chlorinated hydrocarbon, mostly used to make vinyl chloride monomer, the crucial precursor for PVC production (Huang et al., 2014). It is determined to be a probable human carcinogen, and has been listed as a priority pollutant by the U. S. EPA (Pan et al., 2015). In recent years, heterogeneous photocatalys is as an advanced oxidation process (AOP) have attracted considerable attention as a non-selective

Original Article

chemical process for degradation of organic pollutants by oxidation through reactions with hydroxyl radicals (OH•) (Hung et al., 2008). TiO_2 is an n-type semiconductor and PAni is a p-type polymer, the composition of which, as shown in Figure 1, results in reducing band gap energy and hindering recombination (Zhou et al., 2019).

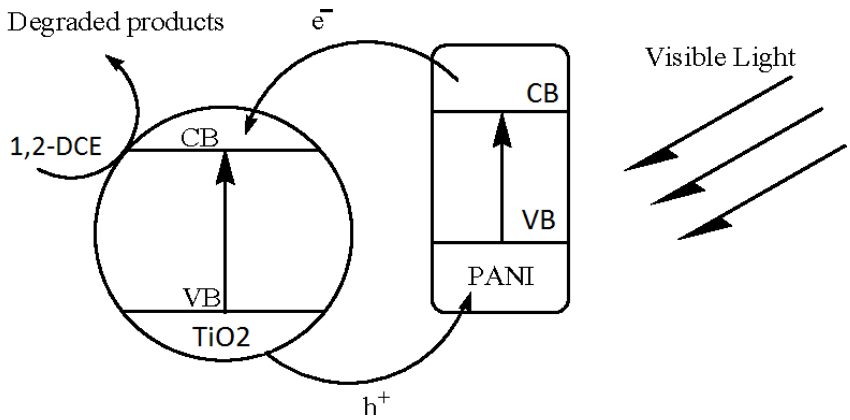

Figure 1: Mechanism of Photocatalytic Degradation of 1, 2-DCE using PAni-TiO2 Nanocomposite

Mechanism of photocatalytic degradation of 1,2-DCE using PAni-TiO_2nanocomposite may be as follows (Salem et al., 2009):

$$PAni-TiO_2+h\nu \rightarrow PAni-TiO_2(e^- + h^+) \tag{1}$$

$$PAni-TiO_2(e^-)+O_2 \rightarrow PAni-TiO_2+O_2^{\bullet -} \tag{2}$$

$$PAni-TiO_2(h^+)+H_2O \rightarrow PAni-TiO_2+h^+ + OH^{\bullet} \tag{3}$$

$$1,2-DCE+OH^{\bullet} \rightarrow CO_2+H_2O+HCl \tag{4}$$

$$1,2-DCE+O_2^{\bullet -} \rightarrow CO_2+H_2O+HCl \tag{5}$$

Photocatalytic processes are complicated, because many independent influential parameters can affect degradation efficiency as the response of the system (Niu et al., 2003). Response surface methodology (RSM) establishes a regression mathematical relationship between independent and response parameters for seeking the optimum conditions of a complicated multivariable system with the lowest number of tests(Somani et al., 1999). The RSM method has been successfully used in various complex processes, including photocatalytic degradation of pollutants using immobilized photocatalysts (Mohammadikish et al., 2013). Artificial Neural Network (ANN) can be considered as a promising modeling technique, because it does not require mathematical equations governing the complicated processes (BagheriAl-jabery et al., 2019). Due to the advantages and disadvantages of both methods, performance of RSM and ANNfor modeling of photocatalytic degradation process have been compared in previous studies (Aghaeinejad-Meybodi et al., 2015; Azadi et al., 2018; Biglarijoo et al., 2017).

In this study, the performance of RSM and ANN models for prediction of 1,2-DCE photocatalytic degradation were compared using the statistical errors including MAE, MSE, RMSE, MAPE, NRMSE and regression coefficient R^2.

2. MATERIALS AND METHODS

2.1 Experimental Procedure

PAni-TiO_2 nanocomposite was synthesized using in-situ deposition oxidative polymerization method. Immobilization of the PAni-TiO_2 nanocomposite on glass beads was carried out by a modified dip coating and heat attachment method. A photo reactor was designed for photocatalytic degradation of volatile organic compounds. Three cylindrical photocatalytic reactors were connected to each other in series by polyethylene tubes (Figure 2). Each reactor consists of three concentric cylinders and a central lamp which enables the reactor to perform either Xenon or UV tests by replacing the lamp.

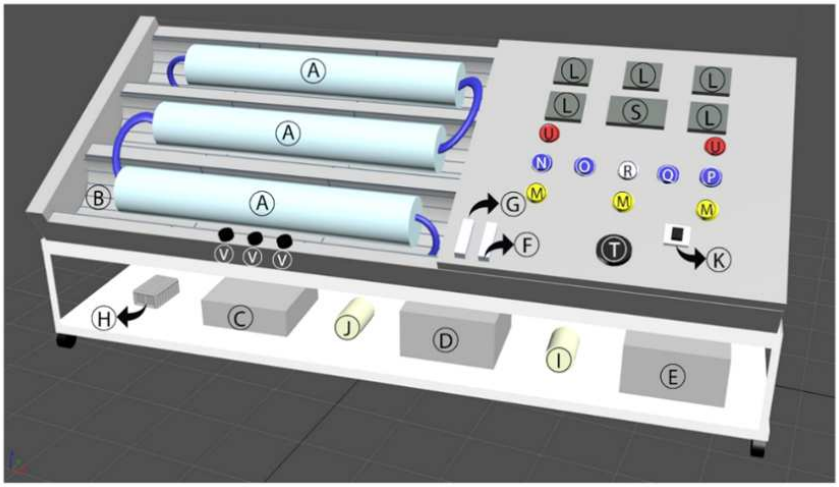

(A) Cylindrical Photocatalytic Reactors
(B) Aluminum Collectors,
(C) Wastewater Tank
(D) Water Tank
(E) Temperature Adjusting Tank
(F) Wastewater Flow Meter
(G) Air Flow Meter
(H) Aeration Pump
(I) Water Pump
(J) Waste Water Pump
(K) Power Switch
(L) Digital Temperature Controller Display, ON/OFF Switches for
(M) Lamps
(N) Waste Water Pump
(O) Water Pump
(P) Mixer
(Q) Water Circulation between Submersible Pumps
(R) Air Pump, (S) Water Level Monitoring
(T) Controller for Heater Temperature
(U) ON/OFF Switch for Heaters
(V) Sampling Port for Each Reactor and
(b) Designed and Built Photocatalytic Reactor

Figure 2: (a) Schematic of the Photocatalytic Reactor Designed and Constructed for Photocatalytic Degradation of 1,2-DCE

Sample collection and preservation was carried out according to standard methods 6010 (APHA, 2012. 1, 2-DCE was analyzed according to standard methods 6200B (APHA, 2012). Gas chromatography analysis was carried out using gas chromatography (Agilent technologies 7890B GC system) with mass selective detector (7955A MSD). All designed experiments were carried out at radiation of a 150W xenon lamp, Wastewater flow of 40 L/h, aeration flow of 2 L/min, initial concentration of 200 mg/l and pH of 7. HCl and NaOH (1M) were used for pH adjustment. For all experiments, after 2 h, a sample was withdrawn to calculate the 1,2-DCE degradation using the following equation:

$$1,2-DCE\ degradation\% = \frac{C_0 - C_t}{C_0} \times 100 \quad (6)$$

Where, $C_0(\frac{mg}{l})$ is the initial concentration of 1,2-DCE at $t = 0$ and $C_t(\frac{mg}{l})$ is the concentration of 1,2-DCE at t.

2.2 Experimental Design

In this research, catalyst composition and catalyst loading were considered as independent parameters. The range and level of these parameters were determined based on preliminary experiments and previous researches. The 1,2-DCE degradation was considered as the response parameter. Central composite design (CCD) was used for design of the experiments and the results are depicted in Table 1.

Table 1: Range and Level of Independent Parameters

Range and Level						
Factors	**Units**	**- α**	**Low (-1)**	**Middle (0)**	**High (+1)**	**+ α**
Catalyst loading	mg/cm^2	0.1	0.2	0.3	0.4	0.5
Catalyst Composition	[TiO_2:PAni]	0.3	1.0	1.7	2.4	3.1

2.3 Response Surface Methodology Modeling

RSM presents a multivariable regression equation to predict the response parameter using the least amount of data. The fitted equation can be a polynomial with a maximum degree of two in the following form:

$$Y_{pred} = \beta_0 + \sum_{i=1}^{k} \beta_i x_i + \sum_{i=1}^{k} \beta_{ii} x_i^2 + \sum_{i\langle j}^{k} \beta_{ij} x_i x_j \tag{7}$$

Where, Y_{pred} is predicted value of the response parameter; β_0 is constant coefficient; β_i is linear effect of the parameter x_i ; β_{ii} is second order effect of the parameter x_i ; and β_{ij} is interaction linear effect of the parameter x_i and x_j. The statistical significance of each β coefficient is investigated using the analysis of variance (ANOVA). If the relationship between independent parameters and the response parameter is linear, β_{ii} and β_{ij} will not be significant, and that should be equal to zero (Sakkas et al., 2010). The results were evaluated using analysis of variance (ANOVA) by Design expert (trial version 10.0.6.0, Stat-Ease Inc.) software.

2.4 Artificial Neural Network Modeling

A multilayer perceptron (MLP) artificial neural network consists of connected artificial neurons grouped into a first layer (independent parameters), one or several hidden layers and one output layer (response parameter). The strength of connections is defined by the weight associated with them (Khataee and Kasiri, 2010). Typically, one hidden layer is sufficient for modeling of any complex process with any desired accuracy (Azadi et al., 2018).

The number of neurons in the hidden layer depends on the complexity of the process being modeled, and is determined by try and error (Gardner and Dorling, 1998). ANN network of this study is shown in Figure 3.

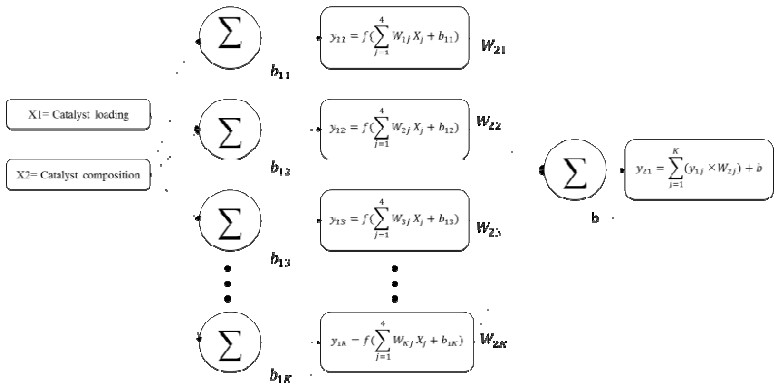

Figure 3: ANN Network of this Study

To select the number of appropriate neurons in the hidden layer of a neural network, valuable guidelines including n/2, n, 2n and 2n + 1, where n is the number of independent parameters, have been given in previous researches (Azadi and Karimi-Jashni, 2016; Bagheri et al., 2015). According to the guidelines, for n=2 (value of n in this study), number of 1, 2, 4 and 5 neurons were recommended respectively. However, these guidelines are not appropriate in all situations. In this study, the number of neurons in the hidden layer was changed from 1 to 9 and resulted neural networks were saved. The tansig and logsig were used as activation functions in the hidden layer and the purelin (linear) function was used in the output layer as follows (Azadi et al., 2018; Khataee and Kasiri, 2010):

$$tansig(x) = \frac{2}{1+e^{-2x}} - 1 \tag{8}$$

$$logsig(x) = \frac{1}{1+e^{-x}} \tag{9}$$

$$purelin(x) = x \tag{10}$$

Bayesian regulation (BR), levenberg marquardt (LM), resilient back propagation (RP) and scaled conjugate gradient (SCG) were used as training functions. Experimental results were normalized to meet algorithm requirements as follows (Azadi and Karimi-Jashni, 2016):

$$x_n = \frac{(x'_{max} - x'_{\min})(x - x_{min})}{(x_{max} - x_{min})} + x'_{min} \tag{11}$$

In this equation, x'_{min} and x'_{max} are the minimum and maximum considered values for normalized data, x_{min} and $x_{max}$are the minimum and maximum values of experimental data, x is the experimental value andx_n is the normalized value.

Back-propagation learning algorithm is sensitive to initial weights (Bagheri Akbari et al., 2019). To solve this problem, each structure of the neural network was trained 40 times using initial random weights and the results were saved. Over fitting is one of the major problems of the neural networks. To solve this problem, early stopping method was performed as follows: The experimental data are divided into training (60%), validation (20%) and test (20%) data sets and the training continued until the validation error increased for six consecutive iterations(Azadi et al., 2016; Bagheri et al., 2016).

2.5 ANN Performance Evaluation

There is no single acceptable statistical error for evaluating the performance of neural networks in all problems (Azadi et al., 2016). Therefore, using different statistical errors alongside each other is recommended in previous studies (Aghaeinejad-Meybodi et al., 2015; Azadi et al., 2016; Azadi and Karimi-Jashni, 2016). In this study, performance of neural networks were evaluated based on statistical errors of mean absolute error (MAE), mean squared error (MSE), root mean square error (RMSE), mean absolute percentage error (MAPE), normalized root mean squared error (NRMSE) and the regression coefficientR^2 as follows (G. Zhang et al., 1998):

$$MAE = \frac{\sum_{i=1}^{n}\left|(P_{pre}^{i} - P_{exp}^{i})\right|}{n} \tag{12}$$

$$MSE = \frac{\sum_{i=1}^{n}(P_{exp} - P_{pre})^2}{n} \tag{13}$$

$$RMSE = \sqrt{\frac{\sum_{i=1}^{n}(P_{pre}^{i} - P_{exp}^{i})^2}{n}} \tag{14}$$

$$MAPE = \frac{1}{n}\sum_{i=1}^{n}\left|\frac{P_{pre}^{i} - P_{exp}^{i}}{P_{exp}^{i}}\right| \times 100 \tag{15}$$

$$NRMSE = \sqrt{\frac{\sum_{i=1}^{n}(P_{pre}^{i} - P_{exp}^{i})^2}{\sum_{i=1}^{n}(P_{exp}^{i})^2}} \tag{16}$$

In which, P_{pre} is the predicted value and P_{exp} is the experimental value. The optimum neural network model is the model with error statistics close to zero and regression coefficient R^2 close to one(Khataee and Kasiri, 2010).

3. RESULTS AND DISCUSSIONS

3.1 RSM Modeling Efficiency

Central composite design, experimental values, RSM predicted values and ANN predicted values for photocatalytic degradation of 1,2-DCE is depicted in Table 2.

Table 2: Central Composite Design and the Experimental and Predicted Results of Photocatalytic Degradation of 1,2-dce

Run	Type	Catalyst Loading mg/cm^2	Catalyst Composition [TiO_2:PAni]	Degradation % (Experimental)	Degradation % (RSM Predicted)	Degradation % (ANN Predicted
1	Factorial	0.4	1	51.231	51.677	51.175
2	Factorial	0.2	2.4	65.163	65.276	65.235
3	Axial	0.3	3.1	74.501	74.526	74.257
4	Center	0.3	1.7	60.432	59.587	59.766
5	Factorial	0.4	2.4	71.304	71.421	71.761
6	Axial	0.5	1.7	66.239	66.097	65.869
7	Factorial	0.2	1	48.528	48.971	48.447
8	Axial	0.3	0.3	38.781	38.476	38.969
9	Center	0.3	1.7	60.025	59.587	59.766
10	Axial	0.1	1.7	57.384	57.246	57.129
11	Center	0.3	1.7	58.863	59.587	59.766

As shown in Table 3, RSM suggested a quadratic model by verifying lack of fit and model summary statistics.

Table 3: Model Summary Statistics

Source	Std. Dev.	R^2	Adjusted R^2	Predicted R^2	PRESS	Remark
Linear	2.00	0.9699	0.9623	0.9162	89.30	
2FI	2.04	0.9726	0.9609	0.9204	84.80	
Quadratic	0.63	0.9981	0.9963	0.9930	7.51	Suggested
Cubic	0.78	0.9983	0.9943	0.9385	65.54	Aliased

The final equation of the RSM model in terms of actual factors is as follows:

$$\text{1,2-DCE degradation} = +37.46540 - 30.01680\times\text{Catalyst Loading} + 14.54316\times\text{Catalyst Composition} + 12.28034\times\text{Catalyst Loading}\times\text{Catalyst Composition} + 52.11265\times\text{Catalyst Loading}^2 - 1.57425\times\text{Catalyst Composition}^2 \quad (17)$$

The adequacy of the model was checked using analysis of variance (ANOVA) statistics and the results were depicted in Table 4. The F-value of 535.78 indicates that the model is significant. Values of Prob> F less than 0.05 shows that the model terms including main, interactions and quadratic terms of independent parameters are significant. Non-significant lack of fit indicates that the model is well fitted. The lack of fit F-value of 0.33 indicates that the lack of fit is not significant relative to the pure error. The pred R-squared of 0.9930 is in reasonable agreement with the adj R-squared of 0.9963. Results showed that the obtained RSM model can be used to predict the experimental data.

Table 4: ANOVA Results for 1,2-DCE Photocatalytic Degradation

Source	Sum of Squares	df	Mean Square	F- Value	Prob> F	Remarks
Model	1063.55	5	212.71	535.78	< 0.0001	significant
A-Catalyst loading	58.75	1	58.75	147.99	< 0.0001	
B-Catalyst composition	974.67	1	974.67	2455.03	< 0.0001	
AB	2.96	1	2.96	7.45	0.0414	
A^2	5.24	1	5.24	13.20	0.0150	
B^2	11.49	1	11.49	28.93	0.0030	
Residual	1.99	5	0.40			
Lack of Fit	0.66	3	0.22	0.33	0.8084	not significant
Pure Error	1.33	2	0.66			
Correction Total	1065.53	10				

Figure 4(a) shows that the RSM model is capable of predicting the experimental values in the range independent parameters of this study. Figure 4(b) indicates that studentized residuals follow a normal distribution.

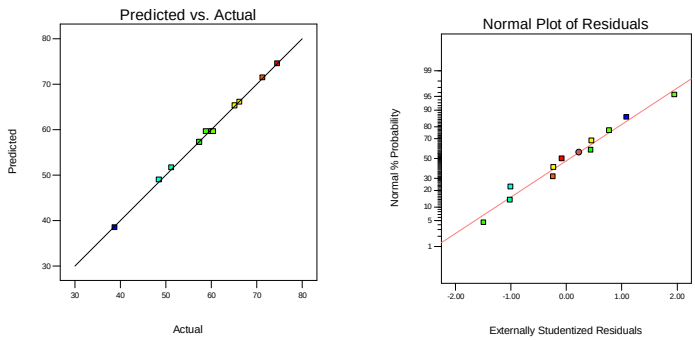

(a) **(b)**

Figure 4: (a) Actual vs Predicted Values and (b) Normal Probability of Studentized Residuals

3.2 ANN Modeling Efficiency

A multilayer perceptron (MLP) network with one hidden layer was developed, in which two input parameters, catalyst loading and catalyst composition were used to predict the 1,2-DCE photocatalytic degradation. For finding the best neural network structure, performance of neural networks with different characteristics including activation function, training function and number of neurons in the hidden layer were evaluated based on five statistical errors of MAE, MSE, RMSE, MAPE, NRMSE and regression coefficient R^2. The best results of training and testing of neural networks for each activation function and training function are presented in the table. In the case of the number of hidden layer neurons, in each activation function and training function, number of 1 to 9 neurons was tested; each neuron with 40 repetitions of network training with initial random weights and the best number of neurons was reported in Table 5. As shown in Table 5, the best network has tansig transfer function, BR training function and two neurons in the hidden layer (2-2-1) with MAE, MSE, RMSE, MAPE, NRMSE and regression coefficient R^2 equals to 0.3228, 0.1679, 0.4097, 0.5374, 0.0068, and 0.9983. Low statistical errors and regression coefficient of 0.9983 indicates that based on the range and level of variables of the present study, artificial neural network was capable to predict 1,2-DCE degradation.

Table 5: Error Statistics of Training and Testing the MLP Neural Network with Different Structures

Acti	Training	Neuron	Train Data Set					Test Data Set				
			Train	Trai	Train	Train	Train	Test	Test	Test	Test	Test
tansi	BR	2- 2- 1	0.360	0.197	0.444	0.597	0.007	0.15	0.03	0.188	0.271	0.003
	LM	2- 3- 1	0.317	0.222	0.471	0.560	0.008	0.19	0.06	0.255	0.329	0.004
	RP	2- 9- 1	0.928	1.160	1.077	1.646	0.019	0.15	0.02	0.158	0.237	0.002
	SCG	2- 5- 1	0.499	0.441	0.664	0.805	0.011	0.15	0.04	0.209	0.235	0.003
logsi	BR	2- 2- 1	0.371	0.212	0.461	0.624	0.008	0.16	0.02	0.167	0.267	0.003
	LM	2- 2- 1	0.376	0.248	0.498	0.613	0.008	0.42	0.30	0.549	0.720	0.008
	RP	2- 3- 1	0.754	0.774	0.880	1.429	0.016	0.58	0.45	0.673	0.983	0.011
	SCG	2- 6- 1	1.574	2.964	1.722	2.496	0.028	0.38	0.20	0.448	0.703	0.007

Early stopping method was used in all developed neural networks of this study to overcome the over fitting problem. The validation set error was monitored until the validation error increased for six consecutive iterations. As shown in Figure 5, training errors are reduced to iteration 73 and then the training of the neural network stopped, and the resulted weights and bias are reported in Table 6.

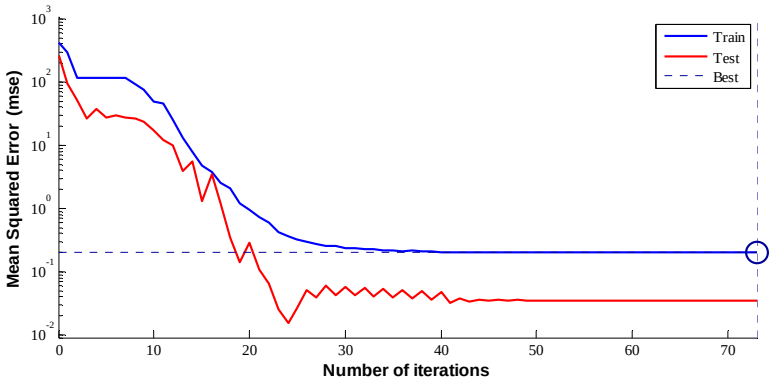

Figure 5: Training and Testing MSE for Optimal ANN Network

Table 6: Weights and Bias of the Optimal ANN Network

Neuron	Weights				Bias
	Variables				
	Catalyst Loading	Catalyst Composition			
1	-0.71	-0.5092			0.5382
2	-0.0968	0.8674			0.487

3.3 Comparison of RSM and ANN Models

The predicted values of RSM and ANN models were depicted in Table. 2. RSM model and the optimum ANN model (tansig, BR, 2-2-1) for 1,2-DCE degradation were compared based on the statistical errors of MAE, MSE, RMSE, MAPE, NRMSE and regression coefficient R^2 and the results are depicted in Table7. As shown in table 7, ANN model with MAE, MSE, RMSE, MAPE, NRMSE and regression coefficient R^2 equals to 0.3228, 0.1679, 0.4097, 0.5374, 0.0068, 0.9983 fitted slightly better to the experimental data than the RSM model. This result is in accordance with previous studies which showed superiority of ANN over RSM (Aghaeinejad-Meybodi et al., 2015; Biglarijoo et al., 2017).

Table 7: Comparison between RSM and Optimal ANN Network

Parameters	RSM Model	ANN Model
MAE	0.3396	0.3228
MSE	0.1804	0.1679
RMSE	0.4247	0.4097
MAPE	0.6139	0.5374
NRMSE	0.0070	0.0068
Regression coefficient R^2	0.9981	0.9983

As shown in Figure 6, although the RSM model deviates more than the ANN model, statistical analysis showed that the difference between the slope of the regression line and the identity line (predicted data = experimental data) for the RSM and ANN models was not statistically significant.

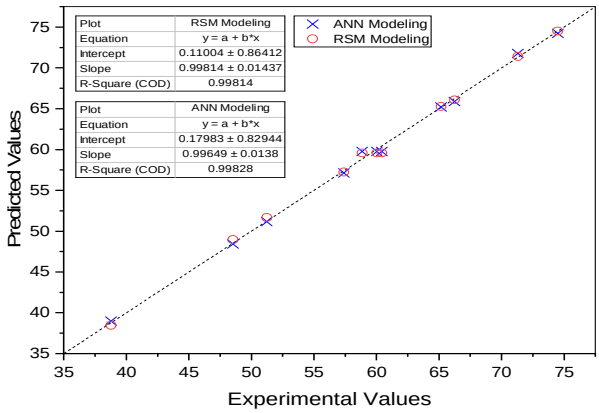

Figure 6: Experimental and Predicted values for the RSM and ANN Models

3.4 Optimization and Confirmation

Numerical optimization was performed by design expert software to find a specific point of the response surface that maximizes the desirability function. The results are depicted in Table 8. The software optimized 1,2-DCE removal (71.42%) by optimizing independent parameters of catalyst loading and catalyst composition at 0.4 mg/cm^{2}and 2.4[TiO_2:PAni], respectively.

Table 8: Results of Numerical Optimization

Name	Goal	Lower Limit	Upper Limit	Lower Weight	Upper Weight	Importance
A:Catalyst Loading	is in range	0.2	0.4	1	1	3
B:Catalyst Composition (TiO2/PAni)	is in range	1	2.4	1	1	3
1,2-dichloroethane Removal	maximize	38.7818	74.5017	1	1	5

Solutions					
Number	Catalyst Loading	Catalyst Composition (TiO2/PAni)	1,2-dichloroethane Removal	Desirability	
1	0.400	2.400	71.422	0.914	Selected
2	0.400	2.395	71.361	0.912	

The confirmation tests were performed in optimized conditions to evaluate the model's accuracy to predict the optimal values of the independent parameters. Table 9 reveals, the average photocatalytic degradation of the confirmation tests was 70.65%, which fell within 95% of the prediction interval bands, which confirmed that the model's accuracy.

Table 9: Confirmation Results

Solution 1 of 2 Response	Predicted Mean	Predicted Median	Observed	Std Dev	n	SE Pred	95% PI low	Data Mean	95% PI high
1,2-dichloroethane Removal	71.4217	71.4217		0.630088	1	0.773951	69.4322	70.65	73.4112

Two-sided Confidence = 95%

3.5 Effect of Independent Parameters on the 1,2-DCE Photocatalytic Degradation

Figure 7(a) illustrated a 3D surface plot of the polynomial, which was obtained from Eq. 17. It is obvious from Contour plot in Figure 7(b) that increasing catalyst loading and catalyst composition increases the degradation efficiency. This is in agreement with results of previous studies (Eydivand and Nikazar, 2015; Sabbaghi et al., 2015). Significant increase in 1,2-DCE degradation was observed due to catalyst composition variation. This finding is in accordance with previous studies that claimed that [PAni:TiO_2] with [1:3] composition had the best photocatalytic degradation efficiency(Sabbaghi et al., 2015; L. Zhang et al., 2006). Variation of Catalyst loading had a lesser effect on 1,2-DCE degradation efficiency. Previous studies indicated that an optimum catalyst loading exists(Chen et al., 2000, 2001; Choi et al., 2001; Yu et al., 2003). It can be argued that with small amounts of catalyst, the photocatalytic degradation efficiency is not high because, the efficiency of light absorption is not sufficient. When catalyst loading increases, light-induced electron-hole pairs created and photocatalytic degradation efficiency increases. Further increase in catalyst loading and decrease in light penetration decreased the amount of light-induced electron-hole pairs. In addition, electron-hole pairs created far from the photocatalyst-substrate interface, which increases the recombination rate. Thus, photocatalytic degradation efficiency decreases(Chen et al., 2001).

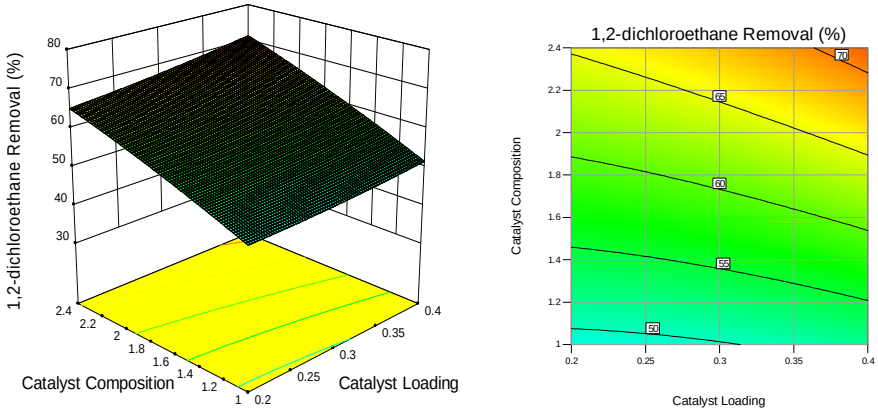

Figure 7: (a) 3D Response Surface and (b) Contour plot for 1,2-DCE Photocatalytic Degradation

4. CONCLUSIONS

In this study, RSM and ANN models were used to predict the 1,2-DCE degradation using catalyst loading and catalyst composition as independent parameters and 1,2-DCE degradation as the response parameter. PAni-TiO_2 nano composite was synthesized with different compositions of TiO_2/PAni (i. e.: 0.3, 1.0, 1.7, 2.4, 3.1) using in-situ deposition oxidative polymerization method. Immobilization of the PAni-TiO_2nanocomposite on glass beads was carried out by a modified dip coating and heat attachment method. ANOVA results showed that pred R-squared of 0.9930 was in good agreement with the adj R-squared of 0.9963 for the proposed quadratic model. RSM model statistical errors of MAE, MSE, RMSE, MAPE, NRMSE and regression coefficient R^2 was 0.3396, 0.1804, 0.4247, 0.6139, 0.0070 and 0.9981. The optimum ANN network had tansig transfer function, BR training function and two neurons in the hidden layer (2-2-1) with MAE, MSE, RMSE, MAPE, NRMSE and regression coefficient R^2 equals to 0.3228, 0.1679, 0.4097, 0.5374, 0.0068, and 0.9983. Comparison of RSM model and the optimum ANN model showed that for the range and level of parameters of the present study, although both models showed good prediction ability, Optimum ANN model possess a slight superiority over RSM model for prediction of 1,2-DCE photocatalytic degradation. The design expert software optimized 1,2-DCE removal (71.42%) by optimizing independent parameters of catalyst loading and catalyst composition at 0.4 mg/cm^2 and 2.4 [TiO_2:PAni], respectively.

ACKNOWLEDGEMENT

This work was financially supported by K. N. Toosi University of Technology. The authors gratefully acknowledge K. N. Toosi University of Technology for supporting this project.

REFERENCES

1. *Aghaeinejad-Meybodi, A., Ebadi, A., et al. (2015). Modeling and optimization of antidepressant drug fluoxetine removal in aqueous media by ozone/H2O2 process: comparison of central composite design and artificial neural network approaches. Journal of the Taiwan Institute of Chemical Engineers, 48, 40-48.*
2. *APHA. (2012). Standard methods for the examination of water and wastewater. American Public Health Association, APHA.*
3. *Azadi, S., Amiri, H., et al. (2016). Evaluating the ability of artificial neural network and PCA-M5P models in predicting leachate COD load in landfills. Waste management, 55, 220-230.*

4. *Azadi, S., & Karimi-Jashni, A. (2016). Verifying the performance of artificial neural network and multiple linear regression in predicting the mean seasonal municipal solid waste generation rate: A case study of Fars province, Iran. Waste management, 48, 14-23.*

5. *Azadi, S., Karimi-Jashni, A., et al. (2018). Modeling and optimization of photocatalytic treatment of landfill leachate using tungsten-doped TiO2 nano-photocatalysts: Application of artificial neural network and genetic algorithm. Process Safety and Environmental Protection, 117, 267-277.*

6. *Bagheri, M., Akbari, A., et al. (2019). Advanced control of membrane fouling in filtration systems using artificial intelligence and machine learning techniques: A critical review. Process Safety and Environmental Protection.*

7. *Bagheri, M., Al-jabery, K., et al. (2019). A deeper look at plant uptake of environmental contaminants using intelligent approaches. Science of the Total Environment, 651, 561-569.*

8. *Bagheri, M., Mirbagheri, S. A., et al. (2015). Modeling and optimization of activated sludge bulking for a real wastewater treatment plant using hybrid artificial neural networks-genetic algorithm approach. Process Safety and Environmental Protection, 95, 12-25.*

9. *Bagheri, M., Mirbagheri, S. A., et al. (2016). Modeling of effluent quality parameters in a submerged membrane bioreactor with simultaneous upward and downward aeration treating municipal wastewater using hybrid models. Desalination and Water Treatment, 57(18), 8068-8089.*

10. *Chen, D., Li, F., et al. (2000). Effect of mass transfer and catalyst layer thickness on photocatalytic reaction. AIChE journal, 46(5), 1034-1045.*

11. *Chen, D., Li, F., et al. (2001). External and internal mass transfer effect on photocatalytic degradation. Catalysis Today, 66(2-4), 475-485.*

12. *Choi, W., Ko, J. Y., et al. (2001). Investigation on TiO2-coated optical fibers for gas-phase photocatalytic oxidation of acetone. Applied Catalysis B: Environmental, 31(3), 209-220.*

13. *Eydivand, S., & Nikazar, M. (2015). Degradation of 1, 2-Dichloroethane in simulated wastewater solution: A comprehensive study by photocatalysis using TiO2 and ZnO nanoparticles. Chemical Engineering Communications, 202(1), 102-111.*

14. *Gardner, M. W., & Dorling, S. (1998). Artificial neural networks (the multilayer perceptron)—a review of applications in the atmospheric sciences. Atmospheric environment, 32(14-15), 2627-2636.*

15. *Huang, B., Lei, C., et al. (2014). Chlorinated volatile organic compounds (Cl-VOCs) in environment—sources, potential human health impacts, and current remediation technologies. Environment international, 71, 118-138.*

16. *Hung, W.-C., Chen, Y.-C., et al. (2008). Synthesis and characterization of TiO2 and Fe/TiO2 nanoparticles and their performance for photocatalytic degradation of 1, 2-dichloroethane. Applied Surface Science, 255(5), 2205-2213.*

17. *Khataee, A., & Kasiri, M. (2010). Artificial neural networks modeling of contaminated water treatment processes by homogeneous and heterogeneous nanocatalysis. Journal of Molecular Catalysis A: Chemical, 331(1-2), 86-100.*

18. *Mohammadikish, M., Davar, F., et al. (2013). Synthesis and characterization of hierarchical ZnS architectures based nanoparticles in the presence of thioglycolic acid. Ceramics International, 39(3), 3173-3181.*

19. *Niu, Z., Yang, Z., et al. (2003). Polyaniline–silica composite conductive capsules and hollow spheres. Advanced Functional Materials, 13(12), 949-954.*

20. *Pan, H., Zhu, S., et al. (2015). Graphene-based photocatalysts for oxygen evolution from water. Rsc Advances, 5(9), 6543-6552.*

21. *Ramírez-Morales, I., Rivero, D., Fernández-Blanco, E., & Pazos, A. (2016). Optimization of NIR calibration models for multiple processes in the sugar industry. Chemometrics and Intelligent Laboratory Systems, 159, 45-57.*

22. *Sabbaghi, S., Mohammadi, M., et al. (2015). Photocatalytic degradation of benzene wastewater using PANI-TiO 2 nanocomposite under UV and solar light radiation. Journal of Environmental Engineering, 142(3), 05015003.*

23. *Sakkas, V. A., Islam, M. A., et al. (2010). Photocatalytic degradation using design of experiments: a review and example of the Congo red degradation. Journal of Hazardous Materials, 175(1-3), 33-44.*

24. *Salem, M. A., Al-Ghonemiy, A. F., et al. (2009). Photocatalytic degradation of Allura red and Quinoline yellow with Polyaniline/TiO2 nanocomposite. Applied Catalysis B: Environmental, 91(1-2), 59-66.*

25. *Somani, P. R., Marimuthu, R., et al. (1999). High piezoresistivity and its origin in conducting polyaniline/TiO2 composites. Synthetic Metals, 106(1), 45-52.*

26. *Sultan, J. A., & Jasim, R. M. (2016). Demand forecasting using artificial neural networks optimized by artificial bee colony. Int J. Manage, Inf. Technol. Eng, 4(7), 77-88.*

27. *Yu, J. C., Ho, W., et al. (2003). Photocatalytic activity, antibacterial effect, and photoinduced hydrophilicity of TiO2 films coated on a stainless steel substrate. Environmental science & technology, 37(10), 2296-2301.*

28. *Zhang, G., Patuwo, B. E., et al. (1998). Forecasting with artificial neural networks:: The state of the art. International journal of forecasting, 14(1), 35-62.*

29. *Zhang, L., Liu, P., et al. (2006). Preparation of PANI–TiO2 nanocomposites and their solid-phase photocatalytic degradation. Polymer Degradation and Stability, 91(9), 2213-2219.*

30. *Zhou, T., Ma, L., et al. (2019). Sandwich-structured hybrids: A facile electrostatic self-assembly of exfoliated titania nanosheets and polyaniline nanoparticles and its high visible-light photocatalytic performance. Journal of Physics and Chemistry of Solids, 125, 123-130.*